# Ribosomal protein L7Ae is a subunit of archaeal RNase P

I-Ming Cho[a,b,c], Lien B. Lai[a,c], Dwi Susanti[d,f], Biswarup Mukhopadhyay[d,e,f], and Venkat Gopalan[a,b,c,1]

Departments of [a]Biochemistry and [b]Molecular Genetics, [c]Center for RNA Biology, Ohio State University, Columbus, OH 43210; and [d]Virginia Bioinformatics Institute, [e]Departments of Biochemistry and Biological Sciences, and [f]Genetics, Bioinformatics and Computational Biology Graduate Program, Virginia Polytechnic Institute and State University, Blacksburg, VA 24061

Edited* by Sidney Altman, Yale University, New Haven, CT, and approved June 11, 2010 (received for review April 23, 2010)

**To the mounting evidence of nonribosomal functions for ribosomal proteins, we now add L7Ae as a subunit of archaeal RNase P, a ribonucleoprotein (RNP) that catalyzes 5′-maturation of precursor tRNAs (pre-tRNAs). We first demonstrate that L7Ae coelutes with partially purified *Methanococcus maripaludis* (*Mma*) RNase P activity. After establishing in vitro reconstitution of the single RNA with four previously known protein subunits (POP5, RPP21, RPP29, and RPP30), we show that addition of L7Ae to this RNase P complex increases the optimal reaction temperature and $k_{cat}/K_m$ (by ∼360-fold) for pre-tRNA cleavage to those observed with partially purified native *Mma* RNase P. We identify in the *Mma* RNase P RNA a putative kink-turn (K-turn), the structural motif recognized by L7Ae. The large stimulatory effect of *Mma* L7Ae on RNase P activity decreases to ≤4% of wild type upon mutating either the conserved nucleotides in this K-turn or amino acids in L7Ae shown to be essential for K-turn binding. The critical, multifunctional role of archaeal L7Ae in RNPs acting in tRNA processing (RNase P), RNA modification (H/ACA, C/D snoRNPs), and translation (ribosomes), especially by employing the same RNA-recognition surface, suggests coevolution of various translation-related functions, presumably to facilitate their coordinate regulation.**

pre-tRNA processing | RPP38 | protein-aided RNA catalysis

RNase P is a $Mg^{2+}$-dependent endoribonuclease that is primarily responsible for catalyzing the removal of the 5′ leaders of precursor-tRNAs (pre-tRNAs) (1–3). Except for some unique organellar variants, RNase P functions in all three domains of life as a ribonucleoprotein (RNP) (1, 2). Although catalysis rests with the essential RNase P RNA (RPR) in all three domains of life (4–6), the RNase P protein (RPP) cofactors play essential roles. In the simple one RPR-one RPP bacterial RNase P, the RPP aids RPR catalysis by enhancing cleavage efficiency and affinity for substrate and $Mg^{2+}$ (7–9). The bacterial RPP has not been found in any archaeal or eukaryal genome (10). Eukaryal (nuclear) RNase P, which comprises an RPR and 9 or 10 RPPs (11, 12), has not been reconstituted from recombinant subunits, thus thwarting efforts to uncover the individual functions of eukaryal RPPs. Archaeal RNase P, with an RPR and four RPPs (all homologous to eukaryal RPPs), has therefore been explored as an experimental surrogate for its so-far-intractable eukaryal cousin (13–16). Although native archaeal RNase P has not been characterized, Western analysis and immunoprecipitation validated these four RPPs (POP5, RPP21, RPP29, and RPP30) as being associated with partially purified *Methanothermobacter thermautotrophicus* (*Mth*) RNase P activity (14). Subsequent structural and biochemical reconstitution studies using recombinant subunits have proven the utility of archaeal RNase P as a model system to dissect the role of multiple protein cofactors in facilitating RNA catalysis (16).

Besides POP5, RPP21, RPP29, and RPP30, weak homologies are evident in the archaeal genomes with three other eukaryal RPPs. The first candidate is Alba, an archaeal chromatin protein, whose family members include human RPP20 and RPP25 (17–19). However, despite weak binding of the *Pyrococcus horikoshii* (*Pho*) Alba to its cognate RPR, it neither affects the cleavage rate nor the temperature optimum of the in vitro reconstituted *Pho* RNase P activity (19). Also, Alba did not copurify with *Mth* RNase P and polyclonal antisera against it failed to immunoprecipitate *Mth* RNase P activity (18).

The second candidate is the archaeal ribosomal protein L7Ae (12 kDa) that displays ∼25% identity to human RPP38 (∼35 kDa); the latter has additional sequences that probably facilitate subcellular localization and protein- or RNA-protein interactions in the eukaryotic context (10, 20, 21). To test if this homology is a coincidence, Fukuhara et al. (20) added *Pho* L7Ae to an in vitro reconstituted *Pho* RNase P (RPR + 4 RPPs). They found that *Pho* L7Ae increased (*i*) the maximal activity temperature from 54 to 72 °C, a temperature similar to that of partially purified native *Pho* RNase P assayed in vitro, and (*ii*) the $V_{max}$ for pre-tRNA cleavage by 5-fold (activities compared at 55 and 65 °C in the absence and presence of L7Ae, respectively) (20). Although they concluded that *Pho* RPR lacked kink-turns (K-turns) (22, 23), the typical binding sites of L7Ae, Fukuhara et al. (20) used gel-shift assays to examine the binding of L7Ae to a series of *Pho* RPR deletion mutants and showed that L7Ae binds with unequal affinities to two different stem-loops in the RPR (Fig. 1*A* and Fig. S1) (20). However, there was no evidence for archaeal L7Ae being associated with RNase P in vivo or for the molecular mechanism underlying its recognition of the RPR.

Most archaeal RNase P variants characterized to date come from the kingdom Euryarchaeota and have been classified into types A and M based on the RPR's secondary structure (24). The type A RPRs are so-called based on their resemblance to the bacterial type A (ancestral) RPRs. Among other changes, type M RPRs (largely from Methanococcales) lack P16, as do eukaryal RPRs (Fig. 1 *A* vs. *B*). This region is the high-affinity binding site of L7Ae in *Pho* RPR, and its absence in type M archaeal and all eukaryal RPRs suggests that a universal role for L7Ae and its homologs in RNase P catalysis must involve another RPR region. Therefore, we used a type M archaeal RNase P to investigate if L7Ae is indeed part of the holoenzyme and to understand how it influences catalysis.

Using purified recombinant subunits, we and others have reconstituted type A and M RNase P from different thermophilic archaeal variants [*Mth*, *Pho*, *Pyrococcus furiosus* (*Pfu*) and *Methanocaldococcus jannaschii* (*Mja*)] (13, 15, 25, 26). Because we expected studies on a mesophilic type M variant to yield results that are also applicable to eukaryal RNase P, we decided to focus on RNase P from *Methanococcus maripaludis* (*Mma*); this choice

Author contributions: I-M.C., L.B.L., D.S., B.M., and V.G. designed research; I-M.C., L.B.L., and D.S. performed research; I-M.C., L.B.L., and D.S. contributed new reagents/analytic tools; I-M.C., L.B.L., D.S., B.M., and V.G. analyzed data; and I-M.C., L.B.L., D.S., B.M., and V.G. wrote the paper.

The authors declare no conflict of interest.

*This Direct Submission article had a prearranged editor.

[1]To whom correspondence should be addressed. E-mail: gopalan.5@osu.edu.

This article contains supporting information online at www.pnas.org/lookup/suppl/doi:10.1073/pnas.1005556107/-/DCSupplemental.

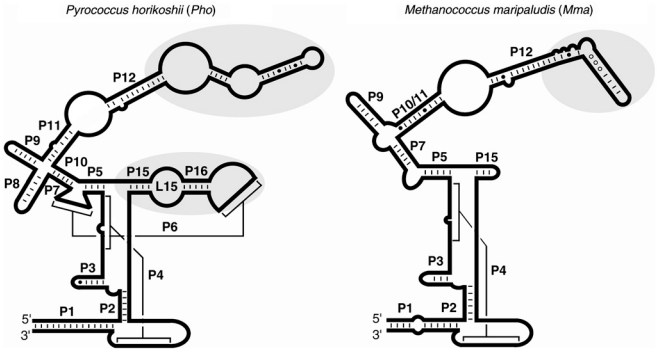


**Fig. 1.** Secondary structure models of *Pho* (type A) and *Mma* (type M) RPR (46). The gray ovals in *Pho* RPR indicate the two possible binding sites for L7Ae identified earlier (20), whereas the one in *Mma* RPR indicates the region investigated in this study (see Fig. 4). Nucleotide sequences of *Pho* and *Mma* RPRs are provided in Fig. S1.

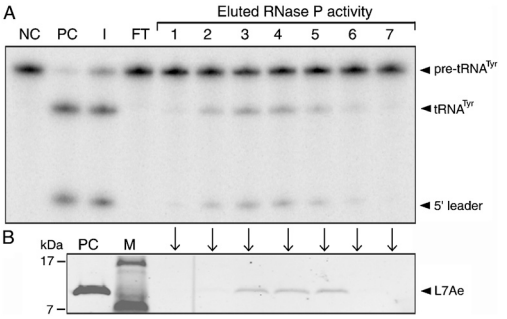


**Fig. 2.** Coelution of *Mma* RNase P activity and L7Ae. (*A*) Partially purified native *Mma* RNase P was assayed for pre-tRNA$^{Tyr}$-processing activity at 37 °C. PC, positive control, generated from processing of pre-tRNA$^{Tyr}$ by in vitro reconstituted *Eco* RNase P. NC, negative control, pre-tRNA$^{Tyr}$ substrate. I and FT, input and flow-through, respectively. (*B*) Western blot analysis of L7Ae from Q-Sepharose fractions of peak activity (*A*) using a rabbit polyclonal antiserum raised against *Mma* L7Ae. PC, positive control, refers to recombinant *Mma* L7Ae. M, size markers.

was also inspired in part by the fact that transformation and homologous recombination are possible for *Mma* (27, 28). By characterizing native *Mma* RNase P, we have now established that L7Ae is indeed a bona fide subunit of RNase P. We also discovered that L7Ae binds a previously unidentified K-turn in *Mma* RPR to elicit a 360-fold increase in the $k_{cat}/K_m$ of *Mma* RNase P. We discuss the evolutionary implications of L7Ae being a member of different archaeal RNPs (RNase P, ribosome, and snoRNPs) involved in translation-related functions.

## Results

**Identification of L7Ae as an Archaeal RPP.** To examine whether L7Ae is an archaeal RPP, we first investigated if L7Ae coelutes with *Mma* RNase P activity. Because L7Ae is also a subunit of the large ribosome, we first separated the ribosomes from RNase P by subjecting clarified *Mma* cell extracts to ultracentrifugation at 100,000 × *g*. Although RNase P was expected in S100 (the supernatant), some activity did appear in P100 (the ribosomal pellet). Therefore, we used a 500-mM NaCl wash to dissociate RNase P from this ribosomal pellet and repeated the ultracentrifugation to obtain the S100* and P100* fractions. Whether we used S100 alone or a pool of S100 + S100* as the starting material for the subsequent purification, similar results for L7Ae coelution were obtained.

RNase P was partially purified from S100 + S100* by ion-exchange chromatography using heparin- and Q-Sepharose sequentially. The Q-Sepharose fractions constituting the peak of RNase P activity are shown in Fig. 2*A*. Protein from these fractions was precipitated with trichloroacetic acid and then subjected to Western blot analysis using a rabbit polyclonal antiserum raised against recombinant *Mma* L7Ae (Fig. 2*B*). The results clearly demonstrate the correspondence of L7Ae in the peak of *Mma* RNase P activity. As an additional confirmation, we constructed by homologous recombination an *Mma* strain BM100 [Δ*hpt* $(His)_6$-HA-RPP30] that has a tandem $(His)_6$-HA (hemagglutinin) tag fused to the N terminus of *Mma* RPP30 (see *SI Text*). The ribosome-free extract from this strain was subjected to partial purification of RNase P using sequential heparin-Sepharose and immobilized metal ($Ni^{2+}$) affinity chromatography (IMAC), which exploited the presence of $(His)_6$-HA-RPP30 in RNase P. Analysis of the IMAC fractions corresponding to the peak of RNase P activity confirmed the coelution of L7Ae with RNase P activity (Fig. S2).

**In Vitro Reconstitution of *Mma* RNase P.** We next investigated whether L7Ae affects the activity of in vitro reconstituted *Mma* RNase P. The four previously identified *Mma* RPPs (POP5, RPP21, RPP29, and RPP30; Table S1) and *Mma* L7Ae were cloned, overexpressed in *Escherichia coli* (*Eco*) and purified to homogeneity using ion-exchange or affinity chromatography (Fig. 3*A*; see *SI Text*). Our previous in vitro reconstitution studies of *Mja* and *Pfu* RNase P revealed that the functional units are not individual proteins but are binary RPP complexes (POP5•RPP30 and RPP21•RPP29) (25, 26). This observation led us to purify these RPP pairs as complexes after their cooverexpression in *Eco*; moreover, RNase P assembled from *Pfu* RPR and RPPs, purified either individually or as binary complexes, exhibits comparable $k_{cat}$ and $K_m$ values (29). While *Mma* POP5 and RPP30 could be cooverexpressed and purified as a heterodimer, the same strategy was not fruitful for *Mma* RPP21 and RPP29 due to unknown reasons. However, we did successfully purify *Mma* RPP21, RPP29, and L7Ae individually (Fig. 3*A*).

We assembled the *Mma* RNase P holoenzyme using in vitro transcribed, folded *Mma* RPR and the four RPPs, with or without L7Ae. The resulting holoenzyme was tested in a standard RNase P assay under optimal buffer conditions for multiple turnover (S/E = 50) with *Eco* pre-tRNA$^{Tyr}$ as the substrate. As expected, *Mma* RPR + 4 RPPs displayed pre-tRNA$^{Tyr}$ processing activity at 37 °C (Fig. 3*B*). Importantly, at the same assay temperature, addition of L7Ae dramatically increased the pre-tRNA$^{Tyr}$ cleavage (Fig. 3*B*), suggesting an important role for L7Ae in influencing *Mma* RNase P activity.

**Kinetic Studies of in Vitro Reconstituted *Mma* RNase P.** We report here the kinetic parameters of an in vitro reconstituted, type M mesophilic archaeal RNase P, in the presence and absence of L7Ae. For cleavage of pre-tRNA$^{Tyr}$ at 37 °C under optimal multiple-turnover conditions, we obtained a $k_{cat}$ of 10 $min^{-1}$ and $K_m$ of 2.6 μM for the *Mma* RNase P holoenzyme made up of RPR + POP5•RPP30 + RPP21 + RPP29 (Fig. 3*C*). Remarkably, addition of L7Ae to this *Mma* RNase P holoenzyme increased the turnover number to 63 $min^{-1}$, and decreased $K_m$ to 0.044 μM, resulting in a $k_{cat}/K_m$ of $2.4 \times 10^7$ $M^{-1}$ $s^{-1}$ (Fig. 3*C*).

*Pho* L7Ae was shown to increase the thermostability of the *Pho* RNase P holoenzyme made up of the RPR and four RPPs (20). As *Pho* is a hyperthermophile, we examined if the mesophilic *Mma* L7Ae also has this attribute. Indeed, while the optimal assay temperature of in vitro reconstituted *Mma* RNase P in the absence of L7Ae is ~36–38 °C, it increased to ~48–50°C in the presence of L7Ae, mirroring the profile obtained with partially purified native RNase P (Fig. S3).

**Identification of L7Ae Binding Site(s) in *Mma* RPR.** L7Ae and its homologs are part of a protein family associated with both archaeal and eukaryal RNPs and bind an RNA motif called the K-turn (22, 23, 30–38). Although thematic variations exist, most K-turns contain two helical stems separated by an asym-

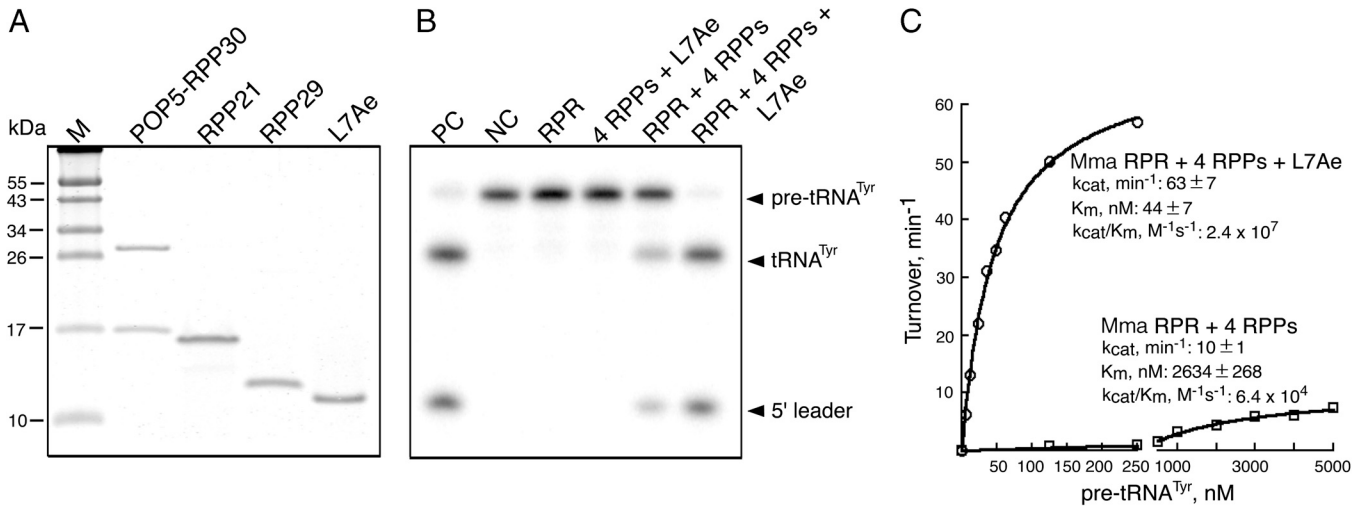


**Fig. 3.** SDS-PAGE analysis of the purity of *Mma* RPPs and L7Ae, and activity of in vitro reconstituted *Mma* RNase P. (*A*) POP5 and RPP30 were purified as a binary complex, and RPP21, RPP29, and L7Ae as individual proteins. (*B*) Reconstitution of *Mma* RNase P with *Mma* RPR, 4 RPPs (POP5, RPP21, RPP29, and RPP30), with or without L7Ae. PC and NC are controls (see legend to Fig. 2*A*). *Mma* RPR (50 nM) was assembled with a 10-fold excess of each protein and assayed with 2500 nM pre-tRNA$^{Tyr}$ for 5 min at 37 °C. (*C*) Michaelis–Menten analysis of reconstituted *Mma* RNase P holoenzymes with or without L7Ae. While representative plots are depicted, the $k_{cat}$ and $K_m$ values reported are the mean and standard deviation from three independent experiments. The curve-fit errors did not exceed 13% ($k_{cat}$) and 26% ($K_m$) in individual trials.

metric 3-nt loop (Fig. 4*A*). Flanking the loop on the 5′ side is a canonical stem with Watson–Crick bps, whereas the 3′ side has two consecutive, sheared GA bps as part of a noncanonical (NC) stem. A sharp kink in the phosphate backbone (the defining feature of this motif) is typically stabilized by proteins and metal ions (32, 39) and results in an interaxial angle of ~60° between the two stems whose nucleotides are now juxtaposed. The diversity of large, cellular RNAs (e.g., rRNA and snoRNAs) that have K-turns attests to this motif's importance in RNA/RNP architecture and function.

To better understand the structure-function relationships of L7Ae in *Mma* RNase P catalysis, we used as a framework the strikingly similar RNA-protein interface revealed by four different high-resolution structures of L7Ae and its homologs bound to their respective K-turn-containing cognate RNA ligands (e.g., C/D box snoRNA, U4 snRNA) (23, 30, 31, 33). In all these cases, a highly conserved NExxK motif in L7Ae homologs permits exquisite structure-specific recognition of the NC stem through H-bonding interactions between the N, E, K side chains and the Gs in the two GA bps. Consistent with this RNA recognition, mutations of the GA bps result in loss of protein binding and function (34, 35). Although its identity is not invariant, the protruding loop nucleotide closest to the NC stem provides additional contacts; in some instances, the O4 carbonyl of the protruding U is within H-bonding distance of the $\varepsilon$-amino group of a conserved Lys, proximal to the NExxK motif in the tertiary fold. This loop nucleotide also engages in hydrophobic interactions and backbone recognition. Chemical/enzymatic probing and gel-shift assays validate the importance of this U (30, 35), because mutating it to C weakens RNA binding, a result easily rationalized by the absence of an O4 carbonyl in C. Collectively, this knowledge of the L7Ae-K-turn interface helped us to design *Mma* L7Ae and RPR mutants.

***Mutagenesis of L7Ae to uncover commonalities in RNA recognition.*** Because the primary sequences of L7Ae family members are highly conserved, we first verified the presence of the NExxK motif in *Mma* L7Ae (Fig. S4) and constructed the mutant *Mma* L7Ae$^{N32A,E33A,K36A}$ to disrupt recognition of the putative K-turn in *Mma* RPR. Indeed, in vitro reconstituted *Mma* RNase P with L7Ae$^{N32A,E33A,K36A}$ displayed only 4% of the activity observed with the wild-type L7Ae (Fig. 5*A*). We confirmed using circular dichroism spectroscopy that the secondary structure of L7Ae$^{N32A,E33A,K36A}$ is not different from that of the wild type (Fig. S5).

***Identifying and validating a K-turn in Mma RPR.*** We searched the *Mma* RPR for the presence of a K-turn motif and identified

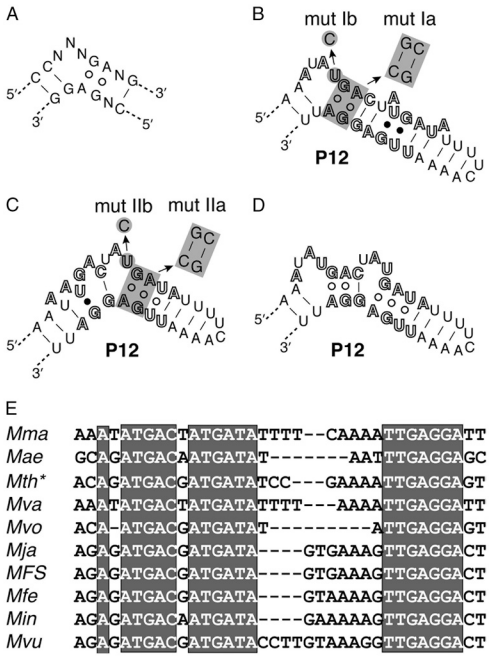


**Fig. 4.** K-turns in *Mma* RPR. A canonical K-turn (*A*) is used as a reference to present different possibilities (*B*, *C*, and *D*) for K-turns in *Mma* RPR that are supported by a sequence alignment of the P12 region of 10 RPRs from Methanococcales (*E*). Mutations used to both validate and discriminate between the possibilities are indicated (*B* and *C*). Conserved nucleotides are outlined (*B*–*D*). (*E*) Currently available Methanococcales RPR sequences from publicly available databases: *Mma* (NC_005791); *Mae*, *Methanococcus aeolicus* (NC_009635); *Mth**, *Methanococcus thermolithotrophicus* (AF192355); *Mva*, *Methanococcus vannielii* (NC_009634); *Mvo*, *Methanococcus voltae* (NZ_ABHB01000002); *Mja* (NC_000909); *MFS*, *Methanocaldococcus* sp. FS406-22 (NC_013887); *Mfe*, *Methanocaldococcus fervens* (NC_013156); *Min*, *Methanocaldococcus infernus* (NC_014122); and *Mvu*, *Methanocaldococcus vulcanius* (NC_013407).

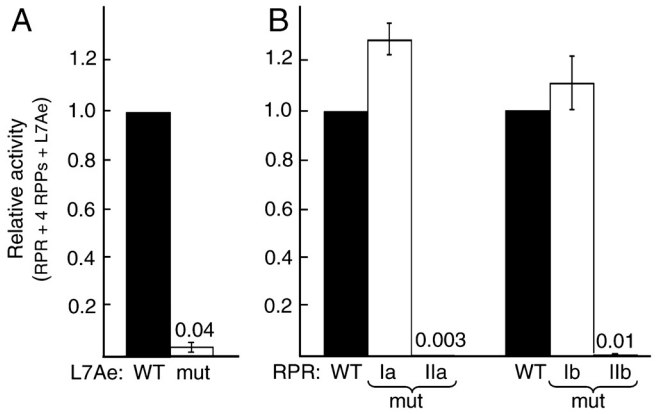


**Fig. 5.** Comparison of the pre-tRNA$^{Tyr}$-processing activity of reconstituted *Mma* RNase P with either the WT or mutant (mut) derivatives of L7Ae or RPR. (*A*) Activity of RPR + 4 RPPs with either WT L7Ae or mut L7Ae$^{N32A,E33A,K36A}$. (*B*) Activity of 5 RPPs reconstituted with either WT or mut RPRs (illustrated in Fig. 4). A turnover number of ~60 min$^{-1}$ for the WT holoenzyme was used as the reference to calculate the relative activities of the different mutants. The mean and standard deviation values were calculated from three independent experiments.

two possible sites in the P12 region based on secondary structure predictions (Fig. 4 *B* and *C*). It is notable that the P12 region in *Pho* RPR harbors a low-affinity binding site for L7Ae (20). Sequence alignment of 10 RPRs from Methanococcales supported both models (Fig. 4*E*). In model I (Fig. 4*B*), the motif differs from the consensus in that it has a 4-nt loop, for which there are precedents (22). In model II (Fig. 4*C*), there is a 3-nt loop with two GA bps on the 3′ side but not a stable (proximal) canonical stem on the 5′ side. We mutated the RPR to discriminate between these two possibilities.

In the a-series mutants, we mutated the two GA bps in each of our two predicted K-turn structures to canonical GC bps (mutants Ia and IIa), whereas in the b series we mutated the loop U to C (mutants Ib and IIb; Fig. 4 *B* and *C*). Using a gel-shift assay, we failed to detect binding of L7Ae to the full-length *Mma* RPR. Therefore, we opted for pre-tRNA cleavage assays to assess the effect of mutating the putative K-turns in the RPR on holoenzyme activity. Strikingly, mutations in the K-turns predicted by models I and II had very different effects on the RNase P activity. When assembled with all five RPPs, the *Mma* RPR mutants Ia and Ib are fully functional, whereas the RPR mutants IIa and IIb show <1% activity (Fig. 5*B*). We attribute this dramatic decrease to the failure of L7Ae to bind RPR mutants IIa and IIb; this premise is confirmed by data from footprinting experiments that revealed the L7Ae-dependent decreased susceptibility of certain P12 positions to RNase T1 cleavage are either absent or greatly reduced with mutant IIa (Fig. S6). Thus, the K-turn predicted by model II is the L7Ae-recognition determinant that is critical for its role in RNase P catalysis.

As expected, the *Mma* RNase P holoenzymes reconstituted with the four RPPs and either wild-type or mutant RPRs (a and b series) showed comparable pre-tRNA$^{Tyr}$ processing activity, indicating no structural aberration in the mutant RPRs that would preclude their interaction with the four RPPs (Fig. S7). These results also rule out the K-turn as being directly recognized by the four RPPs.

## Discussion

**Validating L7Ae as a Subunit of Archaeal RNase P.** L7Ae coelutes with partially purified native *Mma* RNase P activity (wild-type and affinity-tagged versions; Fig. 2 and Fig. S2). It also enhances by ~360-fold the $k_{cat}/K_m$ of the RNP complex reconstituted from the *Mma* RPR and four previously established RPPs (Fig. 3*C*). Notably, the in vitro reconstituted *Mma* RNase P holoenzyme with L7Ae exhibits a $k_{cat}/K_m$ of $2.4 \times 10^7$ M$^{-1}$ s$^{-1}$, a value similar to those reported for native RNase P partially purified from *Mth* (type A) and *Mja* (type M) (40). The presence of L7Ae also increases by ~12 °C the maximal temperature for realizing robust pre-tRNA processing activity of in vitro reconstituted *Mma* RNase P, as reported earlier for *Pho* RNase P (20). Additionally, we have evidence from a heterologous reconstitution assay that *Mma* L7Ae could activate an RNase P holoenzyme assembled from the *Mja* RPR and four RPPs. Collectively, these findings establish L7Ae as a bona fide subunit of archaeal RNase P.

**L7Ae-RPR Recognition in Type M Archaeal RNase P.** *Mma* L7Ae could exert its functional effects on RNase P catalysis either via protein-protein or RNA-protein interactions. A yeast two-hybrid study concluded that *Pho* L7Ae did not engage in protein-protein interactions with POP5, RPP21, RPP29, or RPP30 (41); whether L7Ae interacts with binary RPP complexes has not been determined. Because the ribosomal protein L7Ae binds K-turns, we sought to identify and validate this motif in the secondary structure of *Mma* RPR. Manual examination of 10 different type M RPRs revealed that their respective secondary structures could be drawn to include a K-turn (or K-turn-like) motif at two possible sites in their P12 regions (Fig. 4).

By mutating the tandem GA bps as well as a loop nucleotide vital for L7Ae recognition, we have now proven that the K-turn predicted by model II (Fig. 4*C*) is the L7Ae-interacting site. Some additional lines of evidence support this finding. First, our recent enzymatic footprinting studies place L7Ae at P12 (Fig. S6); because the stable binding of L7Ae appears to require other RPPs, additional work (ongoing) is needed to unambiguously assign this footprint. Second, a low-affinity binding site for L7Ae was shown to be present in the P12 region of *Pho* RPR (20). Third, the initial description of K-turns in rRNAs highlighted this motif in the eukaryal RNase MRP RNA (an RNA evolutionarily related to RNase P RNA) (22); this prediction was subsequently extended to encompass both RNase P and RNase MRP RNAs in a large number of organisms, with the K-turn located in P12 in all cases (10, 42). Fourth, both cross-linking and pull-down experiments using human RNase MRP demonstrated that the putative K-turn-containing region in P12 interacts with RPP38, the L7Ae homolog in human RNase P/MRP (43). Although further experimentation is required, these findings collectively suggest the presence of a K-turn in archaeal and eukaryal RPRs and should motivate studies to uncover common structural motifs in their respective holoenzymes.

We successfully identified the K-turn nucleotides in *Mma* RPR that serve as the L7Ae recognition site. Interestingly, this K-turn (as drawn, Fig. 4*C*) deviates from the consensus in one aspect: The 5′ canonical stem is not a helix made up of contiguous bps but rather appears to have bulges. The recognition of such a structure by L7Ae is consistent with three possibilities. First, archaeal L7Ae binds to both K-turns and K-loops; in the latter instance, the canonical stem is not essential for archaeal L7Ae recognition because a terminal loop replaces the stem (32, 44). Second, L7Ae is part of a multiprotein RNP in RNase P; thus the binding of other RPPs to P12 might somehow enable tolerance of this structural deviation from the consensus. Third, we present an alternative model in which a 5′ stem, albeit comprised of non-canonical bps, flanks the motif recognized by L7Ae (Fig. 4*D*). In fact, 10 different RPRs from Methanococcales can adopt this structure as well (Fig. 4*E*). We are now using both computational and experimental approaches to distinguish between these possibilities.

**Comparing Type A and M RNase P.** The kinetic parameters for *Mma* (type M) RNase P can be compared with those we have reported earlier for *Pfu* (type A) RNase P (26). Without L7Ae, the reconstituted *Mma* RNase P displays a $k_{cat}$ of 10 min$^{-1}$ (at 37 °C)

similar to 9.5 $min^{-1}$ (at 55 °C) for *Pfu* RNase P, but its $K_m$ (2.6 μM) is 14-fold higher than the latter (0.18 μM). While this $K_m$ difference could be attributed to variations in assay conditions (e.g., 37 °C vs. 55 °C assay temperature), it is more likely due to the dissimilarities in RPR structure (Fig. 1) (24). Type M RPRs possess a smaller, atypical L15 and lack P16, P6, and P8; these changes might adversely impact substrate binding, an expectation based on findings from the related bacterial RPR (24, 25). Interestingly, the inclusion of L7Ae lowers the $K_m$ to 0.044 μM for pre-$tRNA^{Tyr}$ processing by *Mma* RNase P. Clearly, RPPs (including L7Ae) somehow remedy the substrate-binding defects of the *Mma* RPR. Elucidating the stoichiometry and exact functional contribution of the individual RPPs in type A and M archaeal RNase P are part of our ongoing studies.

**Evolutionary Perspectives.** L7Ae, a subunit of the large ribosome, plays multiple roles in archaea. It is part of the H/ACA and the C/D box snoRNPs, which catalyze rRNA pseudouridylation and 2′-O-methylation, respectively (34, 35, 37, 38). Through biochemical characterization, we have now confirmed an earlier suggestion that archaeal RNase P should be added to the list of RNPs that contain L7Ae. Specifically, our mutagenesis data permit us to conclude that L7Ae recognizes a K-turn to promote RNase P function, as demonstrated earlier with snoRNPs. L7Ae's multifunctionality may partly be attributable to its using the same RNA-recognition surface to bind similar structures in different RNA ligands and suggests coevolution of these roles. The ribosome, snoRNPs, and RNase P, all of which contain L7Ae in archaea, are linked by their biological function in some aspect of translation. L7Ae's ability to influence the architecture and activity of these distinct RNPs raises the prospect of it playing a role in coordinate regulation, a premise supported by the recent observation that the chaperone Hsp90 might serve as a master control for cell signaling and growth by aiding the biogenesis of human and yeast RNPs containing L7Ae homologs (45).

There is a variable requirement of L7Ae members to nucleate assembly of their resident RNPs. For example, L7Ae binding drives the specificity and affinity for proteins that are subsequently assembled into the C/D box snoRNP (38). In contrast, because a fairly active *Mma* RNase P holoenzyme (made up of the RPR and four RPPs) can be reconstituted even in the absence of L7Ae (Fig. 3), L7Ae is not critical for initiating RNase P assembly, akin to the scenario with H/ACA snoRNP (37). In *Mma* RNase P (Fig. 3*C* and Fig. S3), L7Ae's ability to increase the maximal temperature for activity and decrease the $K_m$ for pre-$tRNA^{Tyr}$ argues that it is a key structural subunit and not merely an accessory chaperone that increases the number of functional holoenzyme molecules assembled. Nevertheless, the possibility remains that L7Ae binding remodels the RPR structure and facilitates high-affinity binding of the other RPPs to the RPR. Consistent with this claim, L7Ae-mediated stabilization of the sharply bent K-turn has been proposed to promote shape/surface features (e.g., exposed base planes) and a strong local electronegative density in the cognate RNA, thereby creating context-dependent platforms for recruitment of other RNA-binding proteins (22, 31). We are attempting to elucidate how L7Ae promotes RPR conformational changes that affect archaeal RNase P assembly and function.

Although eukaryal RNase P does not have L7Ae, it has RPP38, an L7Ae homolog. Replacement of L7Ae with a homolog has also occurred in eukaryal snoRNPs, exemplifying the idea that the emergence of new functions is in part dictated by gene duplication and divergence. There has been a shift from L7Ae, which plays multiple roles in archaea, to diverse and distinctive eukaryal L7Ae homologs, each of which play specific biological roles as part of RNase P, snoRNPs, and snRNPs (34, 36). The driving force for these changes might be the finer regulation and stringent recognition specificity demanded by the complexity of the eukaryotic cell (30, 34, 36).

## Materials and Methods

**Assays for Native and Reconstituted *Mma* RNase P.** RNase P was assayed at 37 °C in 50 mM Tris-HCl (pH 7.5), 500 mM $NH_4OAc$, and 7.5 mM $MgCl_2$ (assay buffer) using *Eco* pre-$tRNA^{Tyr}$ substrate, a trace amount of which was $\alpha$-$^{32}$P labeled. For in vitro reconstitutions, *Mma* RPR was first folded in water by incubating for 50 min at 50 °C, 10 min at 37 °C, and then 30 min at 37 °C in assay buffer. Assembly was initiated by preincubating folded *Mma* RPR, 4 RPPs (POP5, RPP30, RPP21, and RPP29), with or without L7Ae in assay buffer for 5 min at 37 °C, prior to addition of *Eco* pre-$tRNA^{Tyr}$. (*Note*: In the experiment to establish the optimal temperature for maximum activity, an additional 5-min preincubation at the specified temperatures was performed after the preincubation at 37 °C. Assay pH was maintained at the specified temperatures.) Because of the large change in $k_{cat}$ and $K_m$ values upon addition of L7Ae, the reconstituted enzyme with RPR + 4 RPPs + L7Ae (0.625 nM RPR + 31.25 nM of each protein) was assayed with 250 nM of *Eco* pre-$tRNA^{Tyr}$, whereas the RPR + 4 RPPs (50 nM RPR + 500 nM of RPPs) was assayed with 2,500 nM pre-$tRNA^{Tyr}$. The optimal RPR:RPP ratios for each combination were empirically determined. The pre-$tRNA^{Tyr}$ concentration ranges used for measuring the $K_m$ were 6–250 nM for RPR + 4 RPPs + L7Ae, and 62.5–5,000 nM for RPR + 4 RPPs. Turnover numbers were calculated assuming that all of the RPR is assembled into holoenzyme.

All RNase P reactions were quenched after defined incubation periods with urea-phenol dye [8 M urea, 0.04% (wt/vol) bromophenol blue, 0.04% (wt/vol) xylene cyanol, 0.8 mM EDTA, 20% (vol/vol) phenol] and separated on an 8% (wt/vol) polyacrylamide gel containing 8 M urea. The reaction products were visualized by phosphorimaging on the Typhoon (GE Healthcare). The resulting bands were quantitated by ImageQuant (GE Healthcare) to assess the extent of pre-$tRNA^{Tyr}$ cleavage. The initial velocity data were converted to turnover numbers and then subjected to Michaelis-Menten analysis using Kaleidagraph (Synergy Software).

**ACKNOWLEDGMENTS.** We are grateful to Prof. Eric Westhof (Centre National de la Recherche Scientifique, Strasbourg, France) for insightful comments and suggestions. This research was supported by grants from the National Science Foundation (MCB 0843543 to V.G., with subcontract to B.M.) and National Institutes of Health (R01 GM067807, to Mark P. Foster and V.G.).

1. Liu F, Altman S (2010) *Ribonuclease P* (Springer, New York).
2. Lai LB, Vioque A, Kirsebom LA, Gopalan V (2010) Unexpected diversity of RNase P an ancient tRNA processing enzyme: Challenges and prospects. *FEBS Lett* 584:287–296.
3. Walker SC, Engelke DR (2006) Ribonuclease P: The evolution of an ancient RNA enzyme. *Crit Rev Biochem Mol Biol* 41:77–102.
4. Guerrier-Takada C, Gardiner K, Marsh T, Pace N, Altman S (1983) The RNA moiety of ribonuclease P is the catalytic subunit of the enzyme. *Cell* 35:849–857.
5. Kikovska E, Svard SG, Kirsebom LA (2007) Eukaryotic RNase P RNA mediates cleavage in the absence of protein. *Proc Natl Acad Sci USA* 104:2062–2067.
6. Pannucci JA, Haas ES, Hall TA, Harris JK, Brown JW (1999) RNase P RNAs from some Archaea are catalytically active. *Proc Natl Acad Sci USA* 96:7803–7808.
7. Crary SM, Niranjanakumari S, Fierke CA (1998) The protein component of *Bacillus subtilis* ribonuclease P increases catalytic efficiency by enhancing interactions with the 5′ leader sequence of pre-tRNAAsp. *Biochemistry* 37:9409–9416.
8. Sun L, Campbell FE, Zahler NH, Harris ME (2006) Evidence that substrate-specific effects of C5 protein lead to uniformity in binding and catalysis by RNase P. *EMBO J* 25:3998–4007.
9. Sun L, Harris ME (2007) Evidence that binding of C5 protein to P RNA enhances ribozyme catalysis by influencing active site metal ion affinity. *RNA* 13:1505–1515.
10. Rosenblad MA, Lopez MD, Piccinelli P, Samuelsson T (2006) Inventory and analysis of the protein subunits of the ribonucleases P and MRP provides further evidence of homology between the yeast and human enzymes. *Nucleic Acids Res* 34:5145–5156.
11. Chamberlain JR, Lee Y, Lane WS, Engelke DR (1998) Purification and characterization of the nuclear RNase P holoenzyme complex reveals extensive subunit overlap with RNase MRP. *Genes Dev* 12:1678–1690.
12. Jarrous N (2002) Human ribonuclease P: Subunits, function, and intranuclear localization. *RNA* 8:1–7.
13. Boomershine WP, et al. (2003) Structure of Mth11/Mth Rpp29, an essential protein subunit of archaeal and eukaryotic RNase P. *Proc Natl Acad Sci USA* 100:15398–15403.
14. Hall TA, Brown JW (2002) Archaeal RNase P has multiple protein subunits homologous to eukaryotic nuclear RNase P proteins. *RNA* 8:296–306.
15. Kouzuma Y, et al. (2003) Reconstitution of archaeal ribonuclease P from RNA and four protein components. *Biochem Biophys Res Commun* 306:666–673.
16. Lai LB, Cho I-M, Chen W-Y, Gopalan V (2010) Archaeal RNase P: A mosaic of its bacterial and eukaryal relatives. *Ribonuclease P*, eds F Liu and S Altman (Springer, New York), pp 153–172.

17. Aravind L, Iyer LM, Anantharaman V (2003) The two faces of Alba: the evolutionary connection between proteins participating in chromatin structure and RNA metabolism. *Genome Biol* 4:R64.
18. Ellis JC, Barnes J, Brown JW (2007) Is Alba an RNase P subunit? *RNA Biol* 4:169–172.
19. Hada K, et al. (2008) Crystal structure and functional analysis of an archaeal chromatin protein Alba from the hyperthermophilic archaeon Pyrococcus horikoshii OT3. *Biosci Biotechnol Biochem* 72:749–758.
20. Fukuhara H, et al. (2006) A fifth protein subunit Ph1496p elevates the optimum temperature for the ribonuclease P activity from Pyrococcus horikoshii OT3. *Biochem Biophys Res Commun* 343:956–964.
21. Jarrous N, Wolenski JS, Wesolowski D, Lee C, Altman S (1999) Localization in the nucleolus and coiled bodies of protein subunits of the ribonucleoprotein ribonuclease P. *J Cell Biol* 146:559–572.
22. Klein DJ, Schmeing TM, Moore PB, Steitz TA (2001) The kink-turn: A new RNA secondary structure motif. *EMBO J* 20:4214–4221.
23. Vidovic I, Nottrott S, Hartmuth K, Luhrmann R, Ficner R (2000) Crystal structure of the spliceosomal 15.5 kD protein bound to a U4 snRNA fragment. *Mol Cell* 6:1331–1342.
24. Harris JK, Haas ES, Williams D, Frank DN, Brown JW (2001) New insight into RNase P RNA structure from comparative analysis of the archaeal RNA. *RNA* 7:220–232.
25. Pulukkunat DK, Gopalan V (2008) Studies on Methanocaldococcus jannaschii RNase P reveal insights into the roles of RNA and protein cofactors in RNase P catalysis. *Nucleic Acids Res* 36:4172–4180.
26. Tsai HY, Pulukkunat DK, Woznick WK, Gopalan V (2006) Functional reconstitution and characterization of *Pyrococcus furiosus* RNase P. *Proc Natl Acad Sci USA* 103:16147–16152.
27. Moore BC, Leigh JA (2005) Markerless mutagenesis in *Methanococcus maripaludis* demonstrates roles for alanine dehydrogenase, alanine racemase, and alanine permease. *J Bacteriol* 187:972–979.
28. Tumbula DL, Makula RA, Whitman W (1994) Transformation of *Methanococcus maripaludis* and identification of a *Pst* I-like restriction system. *FEMS Microbiol Lett* 121:309–314.
29. Chen W-Y, Pulukkunat DK, Cho I-M, Tsai H-Y, Gopalan V (2010) Dissecting functional cooperation among protein subunits in archaeal RNase P, a catalytic RNP complex. *Nucleic Acids Res,* in press.
30. Charron C, et al. (2004) The archaeal sRNA binding protein L7Ae has a 3D structure very similar to that of its eukaryal counterpart while having a broader RNA-binding specificity. *J Mol Biol* 342:757–773.
31. Moore T, Zhang Y, Fenley MO, Li H (2004) Molecular basis of box C/D RNA-protein interactions; cocrystal structure of archaeal L7Ae and a box C/D RNA. *Structure* 12:807–818.
32. Suryadi J, Tran EJ, Maxwell ES, Brown BA, 2nd (2005) The crystal structure of the *Methanocaldococcus jannaschii* multifunctional L7Ae RNA-binding protein reveals an induced-fit interaction with the box C/D RNAs. *Biochemistry* 44:9657–9672.
33. Hamma T, Ferre-D'Amare AR (2004) Structure of protein L7Ae bound to a K-turn derived from an archaeal box H/ACA sRNA at 1.8 A resolution. *Structure* 12:893–903.
34. Kuhn JF, Tran EJ, Maxwell ES (2002) Archaeal ribosomal protein L7 is a functional homolog of the eukaryotic 15.5 kD/Snu13p snoRNP core protein. *Nucleic Acids Res* 30:931–941.
35. Rozhdestvensky TS, et al. (2003) Binding of L7Ae protein to the K-turn of archaeal snoRNAs: A shared RNA binding motif for C/D and H/ACA box snoRNAs in Archaea. *Nucleic Acids Res* 31:869–877.
36. Watkins NJ, et al. (2000) A common core RNP structure shared between the small nucleoar box C/D RNPs and the spliceosomal U4 snRNP. *Cell* 103:457–466.
37. Charpentier B, Muller S, Branlant C (2005) Reconstitution of archaeal H/ACA small ribonucleoprotein complexes active in pseudouridylation. *Nucleic Acids Res* 33:3133–3144.
38. Omer AD, Ziesche S, Ebhardt H, Dennis PP (2002) In vitro reconstitution and activity of a C/D box methylation guide ribonucleoprotein complex. *Proc Natl Acad Sci USA* 99:5289–5294.
39. Turner B, Melcher SE, Wilson TJ, Norman DG, Lilley DM (2005) Induced fit of RNA on binding the L7Ae protein to the kink-turn motif. *RNA* 11:1192–1200.
40. Andrews AJ, Hall TA, Brown JW (2001) Characterization of RNase P holoenzymes from Methanococcus jannaschii and Methanothermobacter thermoautotrophicus. *Biol Chem* 382:1171–1177.
41. Kifusa M, Fukuhara H, Hayashi T, Kimura M (2005) Protein-protein interactions in the subunits of ribonuclease P in the hyperthermophilic archaeon Pyrococcus horikoshii OT3. *Biosci Biotechnol Biochem* 69:1209–1212.
42. Piccinelli P, Rosenblad MA, Samuelsson T (2005) Identification and analysis of ribonuclease P and MRP RNA in a broad range of eukaryotes. *Nucleic Acids Res* 33:4485–4495.
43. Welting TJ, van Venrooij WJ, Pruijn GJ (2004) Mutual interactions between subunits of the human RNase MRP ribonucleoprotein complex. *Nucleic Acids Res* 32:2138–2146.
44. Tran EJ, Zhang X, Maxwell ES (2003) Efficient RNA 2′-O-methylation requires juxtaposed and symmetrically assembled archaeal box C/D and C′/D′ RNPs. *EMBO J* 22:3930–3940.
45. Boulon S, et al. (2008) The Hsp90 chaperone controls the biogenesis of L7Ae RNPs through conserved machinery. *J Cell Biol* 180:579–595.
46. Brown JW (1999) The Ribonuclease P Database. *Nucleic Acids Res* 27:314.